

High-speed trains: in microchannels?

Jeffrey F. Morris[†]

Levich Institute and Department of Chemical Engineering, CUNY City College of New York, New York, NY 10031, USA



Kahkeshani *et al.* (*J. Fluid Mech.*, vol. 786, 2016, R3) have studied particle ordering in suspension flow in a rectangular microchannel. Experiments and numerical simulations reveal that inertial focusing and hydrodynamic interactions result in long-lived ‘trains’ of regularly spaced particles. The preferred spacing is frustrated at sufficient particle concentration, an important feature for applications.

Key words: microfluidics, multiphase and particle-laden flows, suspensions

1. Introduction

The recent work of Kahkeshani, Haddadi & Di Carlo (2016), hereafter KHD, shows that particles in a microchannel flow can adopt strikingly regular patterns, with many particles moving at nearly fixed axial separation. Phenomena leading to particle ordering are explored, motivated by the utility of ordering in such applications as cell sorting.

As shown by figure 1 (and in movies provided as supplementary material available at <https://doi.org/10.1017/jfm.2016.51>), the particles enter the channel randomly and form lines or ‘trains’ (as described by Matas *et al.* 2004). This structure results from lateral migration combined with hydrodynamic interactions between particles. Lateral migration within the cross-section can be a consequence of particle deformability or non-Newtonian fluid rheology. However, in KHD, the fluid is Newtonian and the particles are undeformed, leaving only inertia to drive migration. Inertial effects may be surprising for microchannel flows, but the low-viscosity liquid (mostly water) yields channel Reynolds numbers of $Re_c = O(100)$.

Inertial migration was described by Segré & Silberberg (1962), who found focusing to a preferred radius, r^* , in a circular tube. The basis for the preferred radius was presented by Ho & Leal (1974), while theory based on a point-particle

[†] Email address for correspondence: morris@ccny.cuny.edu

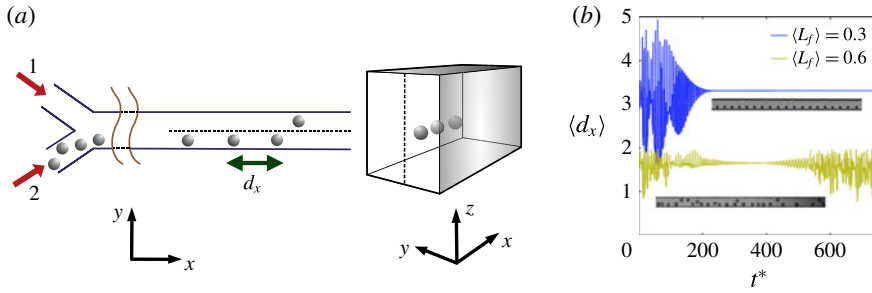


FIGURE 1. (a) Schematic of the microfluidic channel, showing particle entry only from arm 2 at left, and the form of the ordering into trains at right. (b) Relative separation with time and images of particle ordering for different linear densities at $Re_p = 2.8$, showing stable ordering at $\langle L_f \rangle = 0.3$ and loss of stability at $\langle L_f \rangle = 0.6$.

approximation (Schonberg & Hinch 1989) shows that r^* moves toward the boundary with increasing Re_c .

Microfluidic technology has generated interest in non-circular conduits and conditions of strong confinement, for which the particle size is a quite large fraction of the cross-section. In KHD, the particle diameter is fully one-third of the narrow dimension of a rectangular channel. For these conditions, point-particle theories are suspect, and what is known is deduced from experiment and simulation. For example, experiments by Miura, Itano & Sugihara-Seki (2014) show migration in a square channel to focusing points which vary with Re_c , in partial agreement with discrete-particle simulations by Chun & Ladd (2006). A combination of experiments and numerical simulation for rectangular geometries in Humphry *et al.* (2010) was able to capture the evolution to the focusing positions in a rectangular channel, and gave some guidance to the basis for ‘train’ formation. This particle-train formation, and how the particle spacing depends on solid fraction and flow rate, are the subject of KHD.

2. Overview

In KHD, pressure-driven flow is studied in a rectangular channel with dimensions $l_y \times l_z \times l_x = 35 \mu\text{m} \times 60 \mu\text{m} \times 3 \text{cm}$; x is the flow direction as shown in figure 1(a). The particles have diameter $D = 12 \mu\text{m}$ and are highly confined: $D/l_y \approx 1/3$. Variations of behaviour can be described in terms of particle volume fraction, ϕ , and channel Reynolds number, $Re_c = l_y U/\nu$; $\nu \approx 8 \times 10^{-6} \text{m}^2 \text{s}^{-1}$ is the kinematic viscosity of the liquid, and the average axial velocity is $U = 0.7\text{--}2.7 \text{m s}^{-1}$, yielding $Re_c = 30\text{--}120$. The authors use particle Reynolds number $Re_p = (D/l_y)^2 Re_c$, which determines the disturbance flow caused by the particles.

The ordering observed in KHD results first from the tendency to inertially focus due to lateral migration to preferred positions in the cross-section, and second from hydrodynamic interactions (HIs) between particles. The HIs are influenced by inertia and confinement. At small ϕ , the particles focus to the mid-plane in the longer dimension of the cross-section (Z), at locations to either side of the centreline in the other dimension (Y). However, as shown in figure 1(a), the particles enter from only one of two arms entering the channel, so that isolation and ordering are mostly into a single line. It is thus convenient to use the length fraction $\langle L_f \rangle = \langle N \rangle D/L$ with $\langle N \rangle$ the average number of particles within the viewing frame of length L . For $\langle L_f \rangle \approx 0.1$,

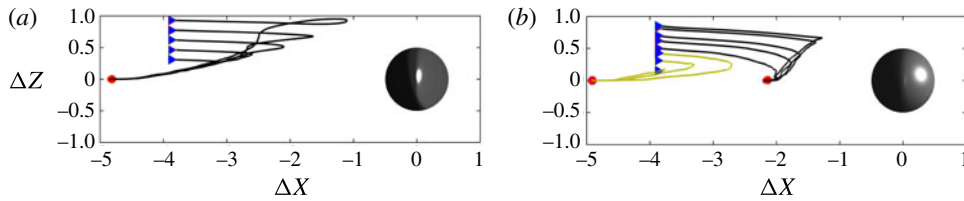


FIGURE 2. Computed trajectories of a second particle released at various separations relative to a first at the focusing point for (a) $Re_p = 2.8$ and (b) $Re_p = 8.3$.

the preferred axial spacing undergoes a transition from $d_x/D \approx 5$ at $Re_p = 2.8$ to $d_x \approx 2.5D$ at $Re_p = 8.3$.

The change in preferred locations was probed using simulations, by the lattice-Boltzmann technique for suspensions (Ladd 1994), of the relative trajectories of particles. While confinement results in flow reversal zones even in Stokes flow (Zurita-Gotor, Blawdziewicz & Wajnryb 2007), the adoption of fixed separations regardless of initial condition requires fluid mechanical nonlinearity, i.e. $Re_p \neq 0$. In figure 2, the trajectories of particles show that at $Re_p = 2.8$, particles starting at a range of positions relative to the first (at the focusing position) all approach, reverse and then move to the same separation: once in this location, the particles occupy the same cross-section location and move together axially at a nearly fixed separation of $d_x/D \approx 5$. At $Re_p = 8.3$, these pair simulations show that particles which start at small Z adopt $d_x/D \approx 5$, whereas those starting at smaller Z move to $2 < d_x/D < 2.5$; intermediate separations are not found. In a many-body system, the presence of a particle at $d_x/D \approx 2.5$ would force a particle which, under isolated-pair conditions, might move to $d_x/D \approx 5$ (relative to the first) to a position of $d_x/D \approx 2.5$ relative to the second, and the process is thus able to order the particles at the fixed smaller separation.

With increase in $\langle L_f \rangle$ (increase of ϕ) at fixed Re_p , d_x/D decreases to accommodate the particles at the focusing position as shown in figure 1(b): $d_x/D \approx 3.2$ for $\langle L_f \rangle = 0.3$ and $Re_p = 2.8$, considerably smaller than $d_x/D \approx 5$ seen at $\langle L_f \rangle = 0.1$. Further increase of the loading to $\langle L_f \rangle = 0.6$ is shown in the same figure to result in a loss of the stable axial order with fluctuating separations.

3. Future

Microfluidic platforms provide a ‘laboratory on a chip’ where scientific experimentation can be performed in remarkably small volumes. A range of basic processes, such as microscale separation (Zhou *et al.* 2014) or mixing, can be performed on-chip. For particle-laden flows, this supports examination of reaction chemistry at particle surfaces or cellular interactions with solution components, among many possibilities.

The work of KHD is motivated by applications in medical diagnostics, where microfluidics has the potential to revolutionize cytometry and cell sorting. In cell sorting, regular arrival times of an ordered train facilitate rapid detection and isolation, supporting high throughput screening to find rare cells. The ordering described in KHD does, however, become more difficult when applied to cell populations, where there is size dispersion and deformability. Evidence for the potential of methods which use both inertia and deformability to discriminate cell populations has been provided by Hur *et al.* (2011), but much is left to be done. Another example is to follow the ordering by encapsulation of the particles (or cells) into drops using

flow focusing, a standard microfluidic element (Anna, Bontoux & Stone 2003) which brings an immiscible sheath fluid around the main stream to cause drop pinch-off. If controlled to each contain one cell, each drop serves as a picolitre to nanolitre environment for a single cell. If ordered particles and ordered cell streams can be combined to have a single particle and a single cell in a drop, assaying tools can be introduced on the particle to deduce the cellular response.

The work of KHD has developed clear understanding of inertial migration and the particle ordering which follows. While applied to a specific geometry, both in terms of channel and confinement ratio, the approach provides a methodology applicable to general conditions. Ultimately, there is a real need for mechanistic understanding of the phenomena involved in inertial microfluidic systems, such that a computed flow of the fluid alone could be used to predict the cross-sectional location of particles. This is presently lacking, but does not seem far out of reach. Such understanding could be used in a description of the particle dynamics in terms of forces on particles immersed in inertial flows in conduits of arbitrary form. Regardless of the form of the tools developed, fully elaborating the fluid mechanical phenomena involved in particle ordering in microchannels will remove a critical hurdle to rational development of a suite of powerful microfluidic methods.

Supplementary movies

Supplementary movies are available at <https://doi.org/10.1017/jfm.2016.51>.

References

- ANNA, S. L., BONTOUX, N. & STONE, H. A. 2003 Formation of dispersions using ‘flow focusing’ microchannels. *Appl. Phys. Lett.* **82**, 364–366.
- CHUN, B. & LADD, A. J. C. 2006 Inertial migration of neutrally buoyant particles in a square duct: an investigation of multiple equilibrium positions. *Phys. Fluids* **18**, 031704.
- HO, B. P. & LEAL, L. G. 1974 Inertial migration of rigid spheres in two-dimensional unidirectional flows. *J. Fluid Mech.* **65**, 365–400.
- HUMPHRY, K. J., KULKARNI, P. M., WEITZ, D. A., MORRIS, J. F. & STONE, H. A. 2010 Axial and lateral ordering in finite Reynolds number channel flows. *Phys. Fluids* **22**, 081703.
- HUR, S. C., HENDERSON-MACLENNAN, N. K., MCCABE, E. R. B. & DI CARLO, D. 2011 Deformability-based cell classification and enrichment using inertial microfluidics. *Lab on a Chip* **11**, 911–920.
- KAHKESHANI, S., HADDADI, H. & DI CARLO, D. 2016 Preferred interparticle spacings in trains of particles in inertial microchannel flows. *J. Fluid Mech.* **786**, R3.
- LADD, A. J. C. 1994 Numerical simulations of particulate suspensions via a discretized Boltzmann equation. Part 1. Theoretical foundation. *J. Fluid Mech.* **271**, 285–309.
- MATAS, J.-P., GLEZER, V., MORRIS, J. F. & GUAZZELLI, É. 2004 Trains of particles in finite-Reynolds number pipe flow. *Phys. Fluids* **16**, 4192–4195.
- MIURA, K., ITANO, T. & SUGIHARA-SEKI, M. 2014 Inertial migration of neutrally buoyant spheres in a pressure-driven flow through square channels. *J. Fluid Mech.* **749**, 320–330.
- SCHONBERG, J. A. & HINCH, E. J. 1989 Inertial migration of a sphere in Poiseuille flow. *J. Fluid Mech.* **203**, 517–524.
- SEGRÉ, G. & SILBERBERG, A. 1962 Behavior of macroscopic rigid spheres in Poiseuille flow. Part 2. Experimental results and interpretation. *J. Fluid Mech.* **14**, 136–157.
- ZHOU, J., GIRIDAR, P. V., KASPER, S. & PAPAUTSKY, I. 2014 Modulation of aspect ratio for complete separation in an inertial microfluidic channel. *Lab on a Chip* **13**, 1919–1929.
- ZURITA-GOTOR, M., BLAWZDZIEWICZ, J. & WAJNRYB, E. 2007 Swapping trajectories: a new wall-induced cross-streamline particle migration mechanism in a dilute suspension of spheres. *J. Fluid Mech.* **592**, 447–469.